Near-Field Leaky-Wave Focusing Antenna With Tapered Dielectric Constant Distribution

Kevin Kipruto Mutai, *Graduate Student Member, IEEE*, Hiroyasu Sato, *Member, IEEE*, and Qiang Chen, *Senior Member, IEEE*

***Abstract*—In this letter, a leaky-wave focusing antenna with a tapered dielectric constant distribution is introduced. The main appeal of the structure is the simplicity and low cost by which the tapering is achieved in the fabrication process where the required effective dielectric constant profile is actualized by three-dimensional printing in less than an hour using the commonly available and inexpensive polylactic acid material. A detailed design method of the structure is presented and the desired focusing effect demonstrated by both simulation and experimental results at Ku-band.**

***Index Terms*—3-D printing, additive manufacturing (AM), antenna synthesis, focusing, leaky-wave antennas (LWAs).**

I. Introduction

THERE has been intense interest into near-field focusing antennas owing to their myriad applications in areas such as RFID readers [1], [2], radiometry [3], hyperthermia [4], [5], and imaging [6]. To address these application needs, several structures have been proposed and leaky-wave focusing antennas (LWFAs) [7], [8], [9], [10], [11], in particular, have been explored owing to their relatively portable physical profile and frequency scanning capability, which greatly simplifies scanning in one dimension.

Despite the stated advantages of the LWFAs, a challenge that remains is the relative fabrication complexity owing to the requirement in tapering the phase constant of the travelling wave along the length of the antenna to achieve the desired focusing effect. This leads to the mechanically complex and financially costly fabrication techniques, such as metal grating [7], mechanically bending the waveguide structure of the antenna [8], [9], tapering of the longitudinal slit [10], or tapering of the broad wall height by CNC machining [11].

To address these fabrication challenges, a LWFA based on the tapering of the dielectric constant within the rectangular waveguide structure of the antenna is proposed in this letter where the required dielectric constant profile is manufactured by the relatively simpler and cheaper 3-D printing process.

Manuscript received 27 December 2022; revised 9 January 2023; accepted 10 January 2023. Date of publication 12 January 2023; date of current version 5 May 2023. This work was supported in part by JSPS KAKENHI under Grant 20K04515 and in part by the Ministry of Internal Affairs and Communications in Japan under Grant JPJ000254. *(Corresponding author: Kevin Kipruto Mutai.)*

The authors are with the Department of Communications Engineering, Graduate School of Engineering, Tohoku University, Sendai 980-8579, Japan (e-mail: mutai-k@ecei.tohoku.ac.jp; sahiro@ecei.tohoku.ac.jp; chenq@ecei.tohoku.ac.jp).

Digital Object Identifier 10.1109/LAWP.2023.3236644

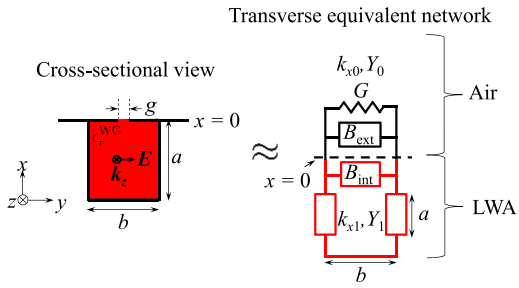

Fig. 1. Cross-sectional view and transverse equivalent network of a rectangular waveguide dielectric-filled LWA.

Though additive manufacturing (AM) has been used to taper the dielectric constant (ε_r) in structures such as lens, reflectarray and dielectric rod antennas [12], to the best of the authors' knowledge this work represents the first time that AM is applied to taper ε_r in LWAs. A generalized design method applicable to LWFAs of similar type (rectangular waveguide-based LWFAs), including the proposed LWFA is treated in Section II. Simulation and experiment results to verify the desired focusing effect are presented in Section III.

II. Design of the Leaky-Wave Focusing Antenna With Tapered Dielectric Constant Distribution

The first step in the design process of the LWFA is to determine the required phase constant distribution ($\beta(z')$) at each position A(z') along the length of the LWFA to achieve focusing at a desired focusing position S(x_s, z_s). This variation in β is such that the radiated field from each point along the length of the antenna converges at the selected focusing position. To achieve this, the tapering of the leaky mode as discussed in [13] is used where the required phase constant distribution is given as

$$\beta(z') = k_0 \frac{z_s - z'}{\sqrt{x_s^2 + (z_s - z')^2}}. \tag{1}$$

The next step is to derive the relationship between β and the physical variable of the rectangular waveguide we wish to taper which in this case is the dielectric constant within the waveguide ($\varepsilon_r{}^{WG}$). When viewed from the transverse direction as indicated in Fig. 1, the physical model of the LWA can be represented by the corresponding network shown [14], [15] where $\varepsilon_r{}^{WG}$

represents the dielectric constant within the waveguide that we wish to taper.

The waveguide narrow wall width is represented by b whereas a represents the broad wall height and the slit width is represented by g. In the equivalent network, k_{xn} and Y_n represent the wavenumber in the x-direction and the admittance at each layer n respectively where $n = 0$ represents the region outside the waveguide ($x > 0$) and $n = 1$ represents the region within the waveguide ($x < 0$). With the reference plane taken as $x = 0$, which coincides with the position of the slit, B_{ext} represents the nonpropagating energy at the top of the slit and B_{int} similarly represents the non-propagating energy at the bottom of the slit. The radiated energy is represented by G. The equation describing the network can therefore be expressed as (from [14], [15])

$$Y_{\text{tot}} = Y_0 + Y_1 = 0. \tag{2}$$

Assuming operation in TE mode

$$Y_0 = \frac{k_{x0}}{\omega\mu_0}(G + jB_{\text{ext}}) \tag{3}$$

$$Y_1 = \frac{k_{x1}}{\omega\mu_0}(-j\cot(k_{x1}a) + jB_{\text{int}}) \tag{4}$$

where

$$k_{x0} = \sqrt{k_0^2 - k_z^2} \tag{5}$$

$$k_{x1} = \sqrt{\epsilon_{\text{r}}^{\text{WG}} k_0^2 - k_z^2} \tag{6}$$

$$G \approx \frac{k_{x0}b}{2} \tag{7}$$

$$B_{\text{ext}} \approx \frac{k_{x0}b}{\pi}\ln\left(\frac{\pi e}{\gamma k_{x0}d}\right) \tag{8}$$

$$B_{\text{int}} \approx \frac{k_{x1}b}{\pi}\ln\left(\frac{\pi g}{2b}\right) \tag{9}$$

in which the constants e and γ are given as 2.718 and 1.781, respectively and k_0 is the wavenumber in free space. To ensure accuracy for a practical design, the loss tangent, tan δ, of polylactic acid (PLA) has also been included in the complex ${\varepsilon_{\text{r}}}^{\text{WG}}$ as 0.01.

After substituting in (3) to (9), (2) was solved for k_z numerically where β and the attenuation constant α can be obtained as the real part and imaginary parts of k_z respectively for different values of a design variable (which in this case was ${\varepsilon_{\text{r}}}^{\text{WG}}$) without having to resort to full-wave simulation software. As we wish to taper the leaky mode where $\beta < k_0$ [15], the limits for the solution of (2) for k_z can be further specified as $0 \le \beta/k_0 \le 1$ and $0 \le \alpha/k_0 \le 1$ for the real and imaginary parts. The dielectric constant ${\varepsilon_{\text{r}}}^{\text{WG}}$ was varied in range $2.0 \le {\varepsilon_{\text{r}}}^{\text{WG}} \le 2.7$ in steps of 0.1 and β was extracted for each value with the results indicated as the solid black lines in Fig. 2. The case of a closed waveguide with $g = 0$ and ${\varepsilon_{\text{r}}}^{\text{WG}} = 2.7$ is also included for reference. It was observed that there is a significant difference between these two cases thereby necessitating the derivation of the leaky-wave antenna (LWA) β as simply using the $g = 0$ case in the design process, though simpler, would result in inaccurate focusing results. The range of ${\varepsilon_{\text{r}}}^{\text{WG}}$ was decided upon because the dielectric material

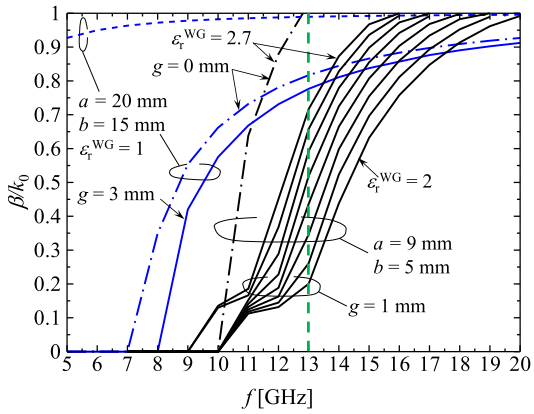

Fig. 2. Frequency characteristics of normalized phase constant of rectangular waveguide air-filled (${\varepsilon_{\text{r}}}^{\text{WG}} = 1$) and dielectric-filled (${\varepsilon_{\text{r}}}^{\text{WG}}$ = variable) LWA.

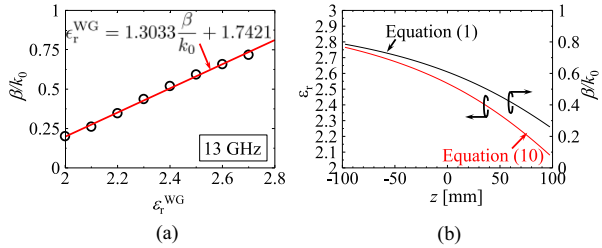

Fig. 3. Relationship between (a) normalized phase constant and waveguide dielectric constant at design frequency of 13 GHz and (b) the required phase constant and the dielectric constant profile to focus on S.

to be used within the waveguide was the commonly available 3-D printer material PLA that has a dielectric constant of about 2.8 [16] in the given frequency range.

By using a dielectric-filled waveguide in solving for (2), an interesting phenomenon observed was that there was only a single solution for β in the stated limits as opposed to an air-filled waveguide where two solutions exist with one solution corresponding to the slot mode [17] that appears between the parallel edges of the longitudinal slit. We may therefore conclude that using a dielectric-filled waveguide can suppress the propagation of the slot mode for the selected design parameters. To confirm this conclusion, β for an air-filled LWA (${\varepsilon_{\text{r}}}^{\text{WG}} = 1$) capable of operating in the same frequency range with $a = 20$ mm, $b = 15$ mm and $g = 3$ mm was calculated and the results indicated as the blue lines in Fig. 2. Two solutions of β in the stated limits were obtained where the dashed and solid lines correspond to the slot and leaky modes, respectively.

From the chart in Fig. 2, the design frequency was selected as 13 GHz. The relationship between ${\varepsilon_{\text{r}}}^{\text{WG}}$ and the normalized β was then derived by interpolation as indicated in Fig. 3(a). The final required ${\varepsilon_{\text{r}}}^{\text{WG}}(z')$ to achieve focusing at S(x_s, z_s) = (195, 150) mm for an antenna of length $L = 200$ mm is therefore derived to be

$$\epsilon_{\text{r}}^{\text{WG}}(z') = 1.3033\frac{\beta(z')}{k_0} + 1.7421 \tag{10}$$

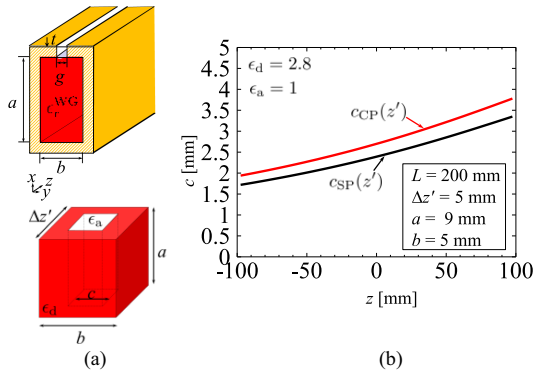

Fig. 4. Unit cell (a) of proposed structure and (b) dielectric constant profiles with circular (c_{CP}) and square (c_{SP}) perforations.

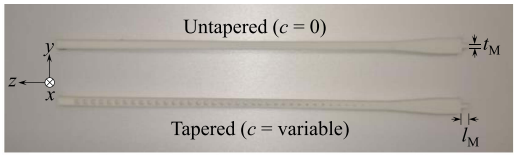

(a)

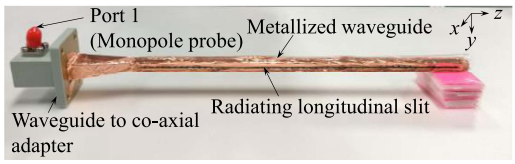

(b)

Fig. 5. Manufactured prototypes of (a) untapered and tapered models without metallization and (b) with metallization by copper tape.

by employing the proposed design method where the $\beta(z')$ obtained in (1) is used and is plotted in Fig. 3(b).

Having derived (10), the perforation profile required to actualize $\varepsilon_r{}^{WG}(z')$ needs to be determined. Either circular (c_{CP}) or square perforations (c_{SP}) [18], [19] can be selected to actualize the effective dielectric constant profile. In this design, a square perforation profile was selected to maximize accuracy by the commercial 3-D printer used and was derived from (3) in [18] and (10) above as

$$c_{SP} = \Delta z' \sqrt{\frac{\epsilon_r^{WG}(z') - \epsilon_D}{\epsilon_a - \epsilon_d}} \tag{11}$$

The result of (11) is plotted in Fig. 4 with the solid dielectric constant $\varepsilon_d = 2.8$ to represent PLA and the perforation dielectric constant $\varepsilon_a = 1$ to represent a hollow perforation. A prototype with the profile given by (11) was fabricated by 3-D printing where the profile took about 40 minutes to produce and is shown in Fig. 5(a) along with an untapered prototype for comparison purposes. The 3-D printing technique used was fused deposition modeling (FDM) owing to the relative popularity and low cost of this technique. It should be mentioned that stereolithography (SLA) 3-D printing [12] techniques can also be used to fabricate the structures in [7], [8], [9], [10], and [11] to reduce the involved fabrication costs. However, due to the mechanisms employed in these structures to taper β, metallization by deposition or electroplating would be necessary to ensure RF performance does not degrade thereby increasing the fabrication complexity. From this perspective, the structure proposed in this work addresses this challenge as the travelling wave is tapered without the mechanical modification of the conducting sections required to support the traveling wave within the waveguide.

TABLE I
COMPARISON OF LWFA MANUFACTURING METHODS

Manufacturing process	$\Delta z'$	Cost	Complexity	Freq. band
[7], [11] CNC machining	$\lambda/5.5$, $\lambda/10$	High	High	X, K bands
[8], [9] Mechanical bending	Smooth	Low	High	X, Ka bands
This letter – FDM 3D printing	$\lambda/2.75$	Low	Low	Ku band

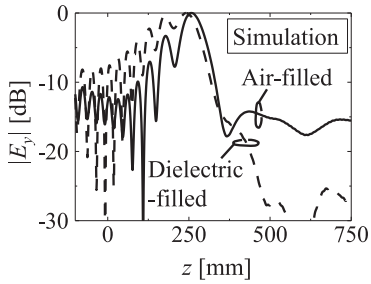

Fig. 6. Simulated electric field distributions along z-direction at $x = 195$ mm for air-filled LWA with $a = 20$ mm, $b = 15$ mm and $g = 3$ mm and dielectric-filled LWA with $a = 9$ mm, $b = 5$ mm, $g = 1$ mm and $\varepsilon_r{}^{WG} = 2.7$.

The models were then simply metallized using adhesive copper tape as shown in Fig. 5(b) and fed by insertion into a WR75 coaxial to waveguide adapter. The section inserted into the adapter has dimensions of $a = 19.05$ mm and $b = 9.525$ mm which is then tapered into the dimensions of the waveguide section of the LWA ($a = 9$ mm, $b = 5$ mm). The combination of 3-D printing and copper taping is significantly cheaper compared to the methods used in [7], [8], [9], [10], and [11] and a comparison of the pros and cons of the fabrication method used in this letter relative to these other structures is given in Table I.

To improve matching between the air region within the adapter and the dielectric-filled region of the metallized waveguide, the matching layer design procedure introduced in [20] was used in which the length of the matching section, $l_M = 5.088$ mm and the thickness, $t_M = 2.7$ mm.

III. SIMULATION AND EXPERIMENTAL RESULTS

To confirm the effect of the slot mode in the near field, an air-filled LWA ($\varepsilon_r{}^{WG} = 1$) and a dielectric-filled LWA ($\varepsilon_r{}^{WG} = 2.7$) with the parameters given in Fig. 2 were calculated using full-wave simulation software. The electric field distribution along the z-direction was then extracted at $x = 195$ mm at 13 GHz for both these structures and is presented in Fig. 6. By observing Fig. 2, it is apparent that at these frequencies the $\varepsilon_r{}^{WG} = 1$ and $\varepsilon_r{}^{WG} = 2.7$ LWAs should have radiation directions, ($\theta_s = \cos^{-1}(\beta/k_0)$), of 39° and 44°, respectively. The difference between these two values is small enough such that the existence

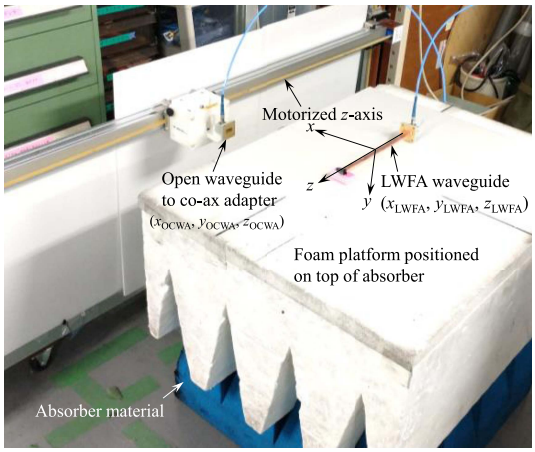

Fig. 7. Experiment setup to measure the electric field distribution of the proposed leaky-wave focusing antenna.

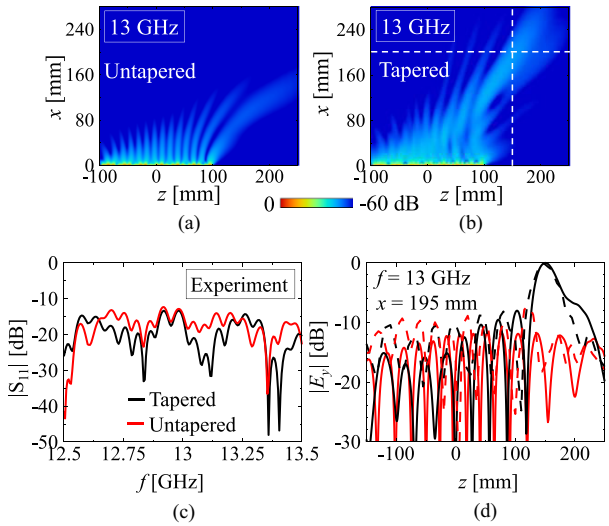

Fig. 8. 2-D simulated electric field distribution for the (a) untapered and (b) tapered models and (c) measured return loss. Simulated and measured electric field distributions (d) along z-direction at $x = x_s = 195$ mm at the design frequency of 13 GHz.

of the slot mode in the radiated field would be readily apparent. From Fig. 6, the air-filled and dielectric-filled LWAs have their main components of the electric filled at around 38° and 43° as expected. The air-filled LWA has an additional strong component at around $z \geq 400$ mm which may be attributed to the slot mode which has an expected $\theta_s \approx 10°$ whereas the dielectric-filled LWA does not have this component thereby validating the conclusion made in Section II regarding suppression of the slot mode and may offer an alternative to the usage of transverse slots as discussed in [17] and [21].

To confirm the focusing effect, a model of the final prototype was calculated using full-wave simulation software and the electric field distribution along the z-direction was extracted at $x = x_s = 195$ mm and the results shown in Fig. 8. From the simulation results indicated in the solid lines, the focusing effect at the desired $S(x_s, z_s) = (195, 150)$ mm at the design frequency of 13 GHz was observed in the tapered case compared to the untapered case thereby lending credence to the design procedure outlined in Section II.

The focusing effect of the fabricated prototype was then confirmed experimentally using the setup shown in Fig. 7 where an open waveguide to coaxial adapter (OCWA), used as a probe, was scanned along the z-direction using a motorized axis at $x = x_s = 195$ mm and the transmission coefficient between the OCWA and the prototype was measured for each position z_{OCWA} and the results shown in Fig. 8(d) as the dashed lines. The return loss of the tapered and untapered structures is shown in Fig. 8(c) where both structures exhibit satisfactory performance. The difference in both cases may be caused by the slight difference in insertion lengths within the adapter feed as well as by variations introduced by the tapering of β.

Good agreement in the focusing effect between the simulation and experimental results was observed with the differences, especially in the low z region (θ_s closer to 90°), being attributed to the scattering from the flat flanges of the probe which is then re-scattered from the antenna under test. A disadvantage in the proposed method is that the 3 dB beamwidth will be reduced compared to the structures presented in [7], [8], [9], [10], and [11] owing to the increased step size ($\Delta z'$) in the tapering of β which is an unavoidable consequence of using a perforation profile owing to the limited tolerances involved compared to other methods such as changing the filling rate [22] along the length of the dielectric which can allow similarly fine $\Delta z'$ as in [7], [8], [9], [10], and [11] (Table I) by using FDM as the smaller the $\Delta z'$, the smaller the 3dB beamwidth and the better the resolution.

IV. Conclusion

In this letter, a LWFA based on the tapering of the ε_r of the rectangular waveguide structure of the antenna was proposed. A generalized design method applicable to structures of a similar nature was presented where the relationship between the β of the travelling wave within the waveguide and the dielectric constant was derived. This relationship was then used to design a perforation profile that was actualized by 3-D printing in a relatively inexpensive, simple, and quick process. The focusing effect was verified by simulation and experiment. Owing to the method of tapering β selected, the structure is limited to submillimeter-wave frequencies as the perforation size is limited by the tolerances of the 3-D printer. Additionally, as the structure is based on the classical leaky-wave antenna, introducing a dielectric into the waveguide means the leaky mode is shifted to lower frequency as β is increased due to the corresponding reduction in wavelength compared to an air-filled waveguide. This challenge, therefore, informs the next steps of this work, which is how to use the proposed concept at higher frequencies, which may necessitate the use of other physical structures such as substrate integrated waveguide or other methods of tapering ε_r without using the perforation profile.

Acknowledgment

The authors would like to thank Dr. X. Cao of Tohoku University for his fruitful technical discussions.

REFERENCES

[1] H.-T. Chou, T.-M. Hung, N.-N. Wang, H.-H. Chou, C. Tung, and P. Nepa, "Design of a near-field focused reflectarray antenna for 2.4 GHz RFID reader applications," *IEEE Trans. Antennas Propag.*, vol. 59, no. 3, pp. 1013–1018, Mar. 2011.

[2] R. Siragusa, P. Lemaitre-Auger, and S. Tedjini, "Tunable near-field focused circular phase-array antenna for 5.8-GHz RFID applications," *IEEE Antennas Wireless Propag. Lett.*, vol. 10, pp. 33–36, 2011.

[3] K. D. Stephan, J. B. Mead, D. M. Pozar, L. Wang, and J. A. Pearce, " A near field focused microstrip array for a radiometric temperature sensor," *IEEE Trans. Antennas Propag.*, vol. 55, no. 4, pp. 1199–1203, Apr. 2007.

[4] J. T. Loane and S. -W. Lee, "Gain optimization of a near-field focusing array for hyperthermia applications," *IEEE Trans. Microw. Theory Techn.*, vol. 37, no. 10, pp. 1629–1635, Oct. 1989.

[5] C. J. Diederich and K. Hynynen, "The feasibility of using electrically focused ultrasound arrays to induce deep hyperthermia via body cavities," *IEEE Trans. Ultrasonics, Ferroelect., Freq. Control*, vol. 38, no. 3, pp. 207–219, May 1991.

[6] K. K. Mutai, H. Sato, and Q. Chen, "Active millimeter wave imaging using leaky-wave focusing antenna," *IEEE Trans. Antennas Propag.*, vol. 70, no. 5, pp. 3789–3798, May 2022.

[7] T. Okuyama, Y. Monnai, and H. Shinoda, "20-GHz focusing antennas based on corrugated waveguide scattering," *IEEE Antennas Wireless Propag. Lett.*, vol. 12, pp. 1284–1286, 2013.

[8] I. Ohtera, "Focusing properties of a microwave radiator utilizing a slotted rectangular waveguide," *IEEE Trans. Antennas Propag.*, vol. 38, no. 1, pp. 121–124, Jan. 1990.

[9] Y. F. Wu and Y. J. Cheng, "Proactive conformal antenna array for near-field beam focusing and steering based on curved substrate integrated waveguide," *IEEE Trans. Antennas Propag.*, vol. 67, no. 4, pp. 2354–2363, Apr. 2019.

[10] J. L. Gomez-Tornero, F. Quesada-Pereira, A. Alvarez-Melcon, G. Goussetis, A. R. Weily, and Y. J. Guo, "Frequency steerable two dimensional focusing using rectilinear leaky-wave lenses," *IEEE Trans. Antennas Propag.*, vol. 59, no. 2, pp. 407–415, Feb. 2011.

[11] T. Hashimoto, H. Sato, and Q. Chen, "Near-field leaky-wave focusing antenna with inhomogeneous rectangular waveguide," *IEICE Commun. Exp.*, vol. 9, no. 6, pp. 1–6, Jun. 2020.

[12] D. Helena, A. Ramos, T. Varum, and J. N. Matos, "Antenna design using modern additive manufacturing technology: A review," *IEEE Access*, vol. 8, pp. 177064–177083, 2020.

[13] P. Burghignoli, F. Frezza, A. Galli, and G. Schettini, "Synthesis of broadbeam patterns through leaky-wave antennas with rectilinear geometry," *IEEE Antennas Wireless Propag. Lett.*, vol. 2, pp. 136–139, 2003.

[14] N. Marcuvitz, "Waveguide handbook," *M.I.T. Radiat. Lab. Ser.*, vol. 10, pp. 183–186, 1951.

[15] L. Goldstone and A. Oliner, "Leaky-wave antennas I: Rectangular waveguides," *IRE Trans. Antennas Propag.*, vol. 7, no. 4, pp. 307–319, Oct. 1959.

[16] M. W. Elsallal, J. Hood, I. McMichael, and T. Busbee, "3D printed material characterization for complex phased arrays and metamaterials," *Microw. J.*, vol. 59, no. 10, pp. 20–34, 2016.

[17] A. Sutinjo, M. Okoniewski, and R. H. Johnston, "Suppression of the slot-mode radiation in a slitted waveguide using periodic slot perturbations," *IEEE Antennas Wireless Propag. Lett.*, vol. 8, pp. 550–553, 2009.

[18] T. Hayat, M. U. Afzal, A. Lalbakhsh, and K. P. Esselle, "Additively manufactured perforated superstrate to improve directive radiation characteristics of electromagnetic source," *IEEE Access*, vol. 7, pp. 153445–153452, 2019.

[19] W. Shao, H. Sato, X. Li, K. K. Mutai, and Q. Chen, "Perforated extensible 3-D hyperbolic secant lens antenna for directive antenna applications using additive manufacturing," *Opt. Exp.*, vol. 29, pp. 18932–18949, 2021.

[20] R. Collin and J. Brown, "The design of quarter-wave matching layers for dielectric surfaces," *Proc. IEE Part C, Monographs*, vol. 103, pp. 153–158, 1956.

[21] T. R. Cameron, A. T. Sutinjo, and M. Okoniewski, "Analysis and design of slitted waveguides with suppressed slot-mode using periodic FDTD," *IEEE Trans. Antennas Propag.*, vol. 60, no. 8, pp. 3654–3660, Aug. 2012.

[22] S. Zhang, R. K. Arya, S. Pandey, Y. Vardaxoglou, W. Whittow, and R. Mittra, "3D-printed planar graded index lenses," *IET Microw., Antennas Propag.*, vol. 10, no. 13, pp. 1411–1419, 2016.